Historical reconstruction of Ocean Acidification in the Australian region

Andrew Lenton[1]
Bronte Tilbrook[1,2]
Richard J. Matear[1]
Tristan P. Sasse[3]
Yukihiro Nojiri[4]

[1]CSIRO Oceans and Atmosphere National Research Flagship, Hobart, Australia
[2]Antarctic Climate and Ecosystems Co-operative Research Centre, Hobart, Australia
[3] Climate Change Research Centre, Kensington Campus, University of New South Wales, Sydney, Australia
[4]National Institute for Environmental Studies, Tsukuba, Japan

1. Abstract

The increase in atmospheric greenhouse gases over the last 200 years has caused an increase in ocean acidity levels. Documenting how the ocean has changed is critical for assessing how these changes could impact marine ecosystems and for the management of marine resources. We use present day ocean carbon observations from shelf and offshore waters around Australia, combined with neural network mapping of CO_2, to estimate the current seasonal and regional distributions of carbonate chemistry (pH and aragonite saturation state). These predicted changes in carbonate chemistry are combined with atmospheric CO_2 concentration changes since to reconstruct pH and aragonite saturation state changes over the last 140 years (1870-2013). The comparison with data collected at Integrated Marine Observing System National Reference Station sites located on the shelf around Australia shows both the mean state and seasonality for the present day is well represented by our reconstruction, with the exception of sites such as the Great Barrier Reef. Our reconstruction predicts that since 1870 an average decrease in aragonite saturation state of 0.49 and of 0.09 in pH has occurred in response to increasing oceanic uptake of atmospheric CO_2. Our reconstruction shows that seasonality is the dominant mode of variability, with only small interannual variability present. Large seasonal variability in pH and aragonite saturation state occur in Southwestern Australia driven

by ocean dynamics (mixing) and in the Tasman Sea by seasonal warming (in the case of aragonite saturation state). The seasonal and historical changes in aragonite saturation state and pH have different spatial patterns and suggest that the biological responses to ocean acidification are likely to be non-uniform depending on the relative sensitivity of organisms to shifts in pH and saturation state. This new historical reconstruction provides an important to link biological observations to help elucidate the consequences of ocean acidification.

2. Introduction

The ocean plays a key role in reducing the rate of global climate change, absorbing approximately 30% of the anthropogenic CO_2 emitted over the last 200 years (Ciais et al., 2013), and more than 25% of current CO_2 emissions (Le Quéré, 2015). The CO_2 taken up by the ocean reacts in seawater, leading to decreases in pH and dissolved carbonate ion concentrations (CO_3^{2-}), these changes being collectively referred to as ocean acidification. Over the past 200 years, it is estimated that there has been a 0.1 unit reduction in the ocean's surface pH, or 26% increase in the concentration of hydrogen ion concentrations in seawater (Doney et al., 2009).

Current projections suggest that the increase in hydrogen ion concentration is likely to be greater than 100% (than the preindustrial period) by the end of the century under high emissions trajectories e.g. Matear and Lenton (2014). Furthermore these changes will persist for many millennia e.g. Frolicher and Joos (2010). Ocean acidification is likely to impact the entire marine ecosystem - from microbial communities to top predators. Factors that can be impacted include reproductive health, organism growth and physiology, species composition and distributions, food web structure and nutrient availability (Aze et al., 2014; Doney et al., 2012; Dore et al., 2009; Fabry et al., 2008; Iglesias-Rodriguez et al., 2008; Munday et al., 2010; Munday et al., 2009).

Aragonite is a metastable form of calcium carbonate that is produced by major calcifiers in coral reef ecosystems, including reef building corals, and is the predominant biogenic carbonate mineral in warm and shallow waters of the tropics (Stanley and Hardie, 1998). The aragonite saturation state of seawater has been used as a proxy for estimating net calcification rates for corals e.g. Langdon (2005).

Projections suggest that by as early as 2050 growth rates of reef building coral may slow to such levels that coral reefs may start to dissolve (Silverman et al., 2009). The impact of acidification combined with other stressors, such as ocean warming, has implications for the health, longer-term sustainability and biodiversity of reef ecosystems (Doney et al., 2012; Dore et al., 2009).

The impact of these changes on the marine environment is fundamental for the management of future marine resources, for nations like Australia with its extensive coastline and regions of international significance such as the Great Barrier Reef. An historical record of the changes that have occurred since the preindustrial period allows us to (i) correctly attribute observed responses over the historical period; (ii) assess how well climate models represent spatial patterns of ocean acidification for the period that overlaps observations (e.g. IPCC AR5); (iii) quantify the magnitude of seasonal and interannual variability, and identify the drivers of this variability; and (iv) provide important boundary conditions for high resolution regional models.

Despite potential impacts of ocean acidification for the Australian region, the number of carbonate chemistry measurements is sparse. The few datasets collected only characterise variability and the mean state in specific environments e.g. (Shaw et al., 2012; Albright et al., 2013) or attempt to synthesize these into regional or habitat-based studies e.g. Gagliano et al. (2010). The only seasonally-resolved observational dataset available to characterize the mean state around Australia in the present day is Takahashi et al. (2014), but this data has coarse resolution and only focuses on the open ocean areas. Studies that have reconstructed the longer-term variability of ocean acidification from coral proxies have been of regional scale and are temporally coarse e.g. Pelejero et al. (2005) and Calvo et al. (2007).

The goals of our study are: (i) reconstruct the observed variability and mean state in pH and aragonite saturation state in the present day around Australia at high spatial resolution and (ii) reconstruct the changes that have occurred in the Australian region over the last 140 years (1870-2013). To this end, we first develop a new salinity-alkalinity relationship for Australian waters based on observations collected around Australia over the last two decades. We then assess our reconstructed pH and

aragonite saturation state fields with data collected around Australia at the Integrated Marine Observing System National Reference Stations (IMOS-NRS; Lynch et al., 2014). Finally, we present the reconstructed aragonite saturation state and pH in the Australian region and discuss the seasonal, interannual and long-term changes in these fields. The reconstructed fields as well as the calcite saturation state, dissolved inorganic carbon dioxide (DIC), total alkalinity (ALK), sea surface temperature and salinity are all available online at http://imos.aodn.org.au.

3. Methods

In this study we focus on the Australian region (Figure 1) delineated nominally by the Subtropical Front (45° S) in the south and the equator (0°) in the north, and between 95°E: 170° E. This region encompasses part of the eastern Indian Ocean and Indonesian Seas and a large part of the Tasman and Coral Seas. The seasonal cycle of physical, chemical, and biological properties of the surface ocean mixed layer this region are described in Condie and Dunn (2006), and will not be described further in this paper. The characterization of the carbon system requires two of six potential carbon parameters (i.e. pH, total dissolved inorganic carbon, total alkalinity, partial pressure of carbon dioxide, bicarbonate, carbonate), from which all the parameters of the ocean carbon system can be calculated. We first use pCO_2 and total alkalinity to reconstruct the changes in ocean acidification.

Oceanic values of pCO_2 were taken from an updated version of Sasse et al. (2013) that used a self-organizing multiple linear output (SOMLO) approach to predict pCO_2 values around Australia on a 1° x 1° degree grid each month for the nominal year of 2000. In brief, the SOMLO approach utilizes the global network of bottle-derived pCO_2 and corresponding standard hydrographic parameters (SHP; temperature, salinity, dissolved oxygen and phosphate; N=17753) to first cluster the dataset into 49 neurons (or bins) based on similarities and homogeneity within the dataset. Principle component regressions were then derived between pCO_2 and the SHP using data within each neuron. This can be thought of as a local-scale optimization, which follows the nonlinear clustering routine. To then predict pCO_2 values for any set of SHP, a similarity measure is first used to establish which neuron best represents the

SHP measurements, once established, pCO_2 values are predicted using the regression parameters of that neuron. Independent testing by Sasse et al. (2013) reveals the SOMLO approach predicts open-ocean pCO_2 values with a global uncertainty of 22.5 µatm (RMSE; N=17350), which decreases to 16.3 µatm (RMSE; N=859) within the Australia region. Monthly pCO_2 climatologies presented in Sasse et al. (2013) were derived using the World Ocean Atlas (WOA) 2009 product (Antonov et al., 2010; Garcia et al., 2010a; Garcia et al., 2010b; Locarnini et al., 2010), which we update here via the WOA 2013 product (Garcia et al., 2014a, b; Locarnini et al., 2013; Zweng et al., 2013). We note that these pCO_2 values provide significantly higher spatial data coverage than the global climatology of Takahashi et al. (2009).

To extend the oceanic pCO_2 values into the past and the future, the value of ΔpCO_2 ($pCO_{2air} - pCO_{2sea}$) was first calculated using Sasse et al. (2013) for the year 2000. This ΔpCO_2 value was then transformed into a time series of oceanic pCO_2 between 1870 to 2013, by adding this to the observed atmospheric CO_2 value over this period using the atmospheric history constructed by Le Quéré et al (2015).

As only limited measurements of total alkalinity (ALK) exist in the Australian region, we develop and use the relationship between ALK and salinity to estimate ALK in the Australian region. While many studies have quantified this relationship globally e.g. Takahashi et al. (2014) and Lee et al. (2006) and regionally e.g. Kuchinke et al. (2014), to date no specific relationship has been developed for the entire Australian region.

To develop this relationship 2772 concomitant measurements of salinity and alkalinity collected in the Australian region over the last two decades were used. (Table 1; Figure 1). From this data we determined our alkalinity-salinity relationship to be:

$$ALK\ (\mu mol/kg) = (2270.0 \pm 0.1) + (64.0 \pm 0.3) * (SAL - 35.) \qquad (1)$$

This relationship is based on a type 2 linear regression, accounting for uncertainty in both the salinity and ALK measurements of 0.05 and 3 µmol/kg respectively. This new relationship was applied to the climatology of salinity (0.5° x 0.5°/daily) taken from the CSIRO Atlas of Regional Seas 2012 (CARS; Ridgway et al., 2002) as no

long-term high spatial and temporal resolution observations of ocean surface salinity at present exist around Australia (nor globally). Nevertheless, based on sparse measurements Durack and Wijffels (2010) suggested that there has been amplification of the global hydrological cycle that has resulted in surface salinity changes over the last 50 years. Their estimated changes around Australia are not uniform and are typically less than ± 0.1, which introduces only a 6.4 μmol/kg change in ALK for the 50-year period. The influence of the changes on the carbonate chemistry (pH and aragonite saturation state changes of about 0.001 and 0.02 respectively), are small compared to the changes predicted from increasing atmospheric CO_2 thereby allowing us to assume that the CARS salinity used has not changed in our calculations.

Sea surface temperature (SST) measurements from 1870 to the present day were obtained from the HadiSST v1.1 dataset (1°x1°; Rayner et al., 2003). Higher resolution datasets do exist, e.g. NOAA OI V2 (0.25° x 0.25°; Reynolds et al., 2007), but none have estimates beyond the last 3 decades, and we chose the 1°x1° product to extend our reconstruction back to pre-industrial period.

We first calculated DIC from TALK, SST and pCO_2 in the period 1870-2013, using the method of Lenton et al., (2012) that used the dissociation constants from Mehrbach et al. (1973) refitted by Dickson and Millero (1987). Our implementation of carbonate chemistry is derived from the OCMIP3 framework (O. Aumont, C. Le Quéré, and J. C. Orr, NOCES Project Interannual HOWTO, 2004, available at http://www. ipsl.jussieu.fr/OCMIP/).

This approach calculates the magnitude of the seasonal cycle of DIC, rather than pCO_2. The pCO_2 seasonality changes over time in response to changes in the Revelle factor and will influence the air-sea gradient in pCO_2, which drives net flux across the air-sea boundary e.g. Hauck and Völker (2015). To correct for this, we first calculated the (detrended) seasonal anomaly of DIC in the period 1995-2006. We then added this seasonal cycle of DIC to the (deseasonalised) long-term DIC record (1870-2013). This allows us to reconstruct the historical DIC fields and the changes in the magnitude of the oceanic pCO_2 in response to the Revelle Factor to be captured.

We then added this seasonal cycle to the deseasonalised long-term DIC record (1870-

2013) to reconstruct the DIC fields, thereby allowing pCO_2 to change. The reconstructed DIC fields were then used in conjunction with our derived alkalinity fields to calculate changes in ocean acidification in the period 1870-2013. As the resolution of SST and pCO_2 fields are nominally 1°x1° monthly fields, all values were calculated on a 1°x1° grid at in-situ temperatures. The values of pH are calculated using the total scale following recommendations of Riebesell et al. (2010) while aragonite and calcite saturation states were calculated following Mucci (1983). To assess the uncertainty in the reconstructed ocean acidification values, we compared these with the values calculated from individual cruises, this allowed us to estimate the uncertainty (as the root mean squared error) to be 0.02 and 0.1 in pH and aragonite saturation state respectively.

4. Results and Discussion

4.1 Assessment of the mean state and seasonal variability at coastal NRS sites

The ability of our reconstruction to predict the mean state and seasonality of ocean acidification around Australia is evaluated by comparing our calculated aragonite saturation state and SST data with carbonate chemistry and SST measurements made over the last few years from seven of the eight Australian IMOS-NRS sites (Figure 2; https://imos.aodn.org.au). The Darwin NRS site was not used in the comparison due to the small number of measurements at this site. To assess how well the observed response at the NRS sites were captured, we calculated both the correlation coefficient (R) and the bias (or bias function) (Table 2).

The observed responses from the NRS sites compared with HadiSST are shown in Figure 3. There is a good correlation in SST at all sites ($r > 0.84$, Table 2) providing confidence that HadiSST represent the character of the seasonal variability. While HadiSST captures the SST variability there were some biases in the mean SST value (Table 2). These biases, e.g. Rottnest Island, likely reflect local process in the coastal environment at the NRS e.g. Lima and Wethey (2012) that are poorly represented by the much larger spatial scale of the HadiSST product.

The reconstructed aragonite saturation state (Ω_{AR}) show good agreement with values calculated from observations (Figure 4). The implication is that the salinity - total alkalinity relationship and calculated pCO_2 fields, which are derived mostly from

offshore data, are valid for most of the IMOS-NRS sites, which tend to be located on the outer shelf. Exceptions are the Ningaloo and Yongala sites, where our reconstruction overestimates the observed values of aragonite saturation state while SST agrees well with HadiSST (Table 2). The total alkalinity -salinity relationship may not hold at these two sites due to the influence of net calcification on nearby coral reef systems and possibly sediment-water exchange that could alter the total alkalinity e.g. Shaw et al. (2012).

Apart from the offsets at the Yongala and Ningaloo sites, the reconstructed aragonite saturation state do recreate the range determined at most locations (e.g. Maria Island, Port Hacking, Rottnest, and North Stradbroke Island). Limited sampling at Kangaroo Island, Esperance and Ningaloo sites prevent direct comparisons of the seasonal variability although the reconstructed variability is plausible based on available measurements.

Overall the ability of our reconstruction to capture the mean state and variability of ocean acidification at the IMOS-NRS sites, gives us confidence in the reconstruction of ocean acidification in the shelf and offshore waters around Australia, and to extend back in time.

4.2 Annual mean state

The mean state of aragonite saturation state around Australia for the period 2000-2009 is shown in Figure 5. The mean state shows a strong latitudinal gradient in aragonite saturation increasing from values of 1.8 in the southern part of the domain to values greater than 3.9 across Northern Australia and into the Coral Sea. The Coral Sea and Western Pacific form part of the coral triangle, a globally significant region in terms of coral and marine diversity (Bell et al., 2011). We see that our reconstructed values in the Coral Sea and into the Western Pacific are also consistent with the observational values of 3.9 calculated by Kuchinke et al. (2014) in this region. This value is well above 3.5, considered to be a key threshold at which corals move from healthy to marginal conditions (Guinotte et al., 2003).

Ricke et al. (2013), using results from an ensemble of CMIP5 simulations and

GLODAP data reported that in the Coral Sea, the present-day values of aragonite saturation state are much less than the 3.5 threshold (Guinotte et al., 2003). These differences are explained by the correction of CMIP5 simulations to GLODAP DIC and ALK values (Key et al., 2004) that have very few measurements in this region.

The annual mean state of pH for the period 2000-2009 is shown in Figure 5. In contrast with aragonite saturation state there is an increasing latitudinal gradient from ~8.1 in Northern Australia to ~8.14 in Southern Australia. The reconstructed values show good agreement on the southern Papua New Guinea coast with Milne Bay observations of Fabricius et al. (2011). However, south of Australia, the pH decreases again to values comparable with those seen in Northern Australia.

The spatial gradients of pH and aragonite saturation state as function of latitude are consistent with the gradients calculated from observations of carbonate chemistry from GLODAP (Key et al., 2004). The distribution of aragonite saturation state is set by both the large-scale distribution of SST, which shows a strong latitudinal gradient, and ALK. Consequently the spatial differences between aragonite saturation state and pH are driven by temperature e.g. Zeebe and Wolf-Galdrow (2001).

4.3 The Seasonal Cycle

The seasonal standard deviation (2-sigma) of aragonite saturation state and pH reveal large spatial differences in the magnitude of the seasonal variability (Figure 5, lower panels). Large seasonality in aragonite saturation state is evident, > 0.4 units. This spatial pattern of this seasonality is quite heterogeneous, with the largest variability occurring along the East Coast of Australia, in the Tasman Sea, and off Southern Australia. The low seasonal variability predicted in the Coral Sea means that aragonite saturation state is above 3.5 even in the winter months. Strong and heterogeneous seasonality in pH is also present, > 0.06 units, around Australia, with the largest range in Southern Australia.

The locations of large seasonality in aragonite saturation state and pH off Southern Australia are associated with regions of deep winter mixing >200m (Condie and Dunn, 2006). Here, the seasonal deepening of the mixed layer in winter supplies

carbon, alkalinity and nutrients to the surface ocean, which in turn alter the chemistry of the surface waters inducing large seasonal variability in ocean acidification values in the surface ocean. That the large seasonal variability in aragonite saturation state is not associated with large seasonal variability in pH along the East Coast of Australia and in the Tasman Sea, suggests that the dominant driver of seasonality variability is SST rather than ocean dynamics, as evident in other regions.

An important consequence of the uncoupling of the pattern of pH and aragonite saturation state is that the biological responses to ocean acidification at the seasonal scale may shift as the susceptibility to pH and aragonite saturation varies between organisms. This has implications for understanding ecosystem responses to ocean acidification.

Small areas of large seasonal variability are also present along parts off northern Australia and off Papua New Guinea. These are primarily driven by large seasonal changes in sea surface salinity driving changes in total alkalinity and DIC which influences the pH and aragonite saturation state.

4.4 Comparison with Takahashi et al (2014)

In this section the reconstructed annual mean and seasonality of pH and aragonite saturation state are compared with that calculated for 2005 (Takahashi et al., 2014); hereafter-denoted T14 (Figure 6). The data of T14 are based on oceanic pCO_2 measurements and regional potential alkalinity versus salinity relationships, at a resolution of 4°x5°. Since T14 excludes Equatorial Pacific (north of 8°S) data and coastal data, we can only compare our results T14 away from these regions.

The T14 spatial pattern of annual mean of aragonite saturation state appears to be in reasonable agreement with our reconstruction for most waters around Australia. An exception is off Northwestern Australia where the mean aragonite saturation state of T14 appears to be an under-estimate. Large differences in the seasonal changes also occur off the east coast of Australia and to the South of Australia. The magnitude of the seasonal variability (in T14) is lower than our reconstruction.

317 The pH values of T14 and our reconstruction both show the highest values in the
318 subtropical waters, although T14 mean values are higher off eastern Australia and
319 lower to the South of Australia. Overall there is quite poor agreement in both the
320 magnitude and spatial pattern of pH variability for most regions.

321 That the spatial pattern of seasonal cycle of aragonite state is not reproduced along the
322 East Coast of Australia and in the Tasman Sea and the variability in Southern
323 Australia is not seen in either pH nor aragonite saturation state suggested that while
324 the seasonal response of SST is captured in T14, the seasonal ocean dynamics are not
325 well represented. Furthermore the underestimation of the magnitude of the seasonal
326 cycle, particularly in regions in which the pattern of the seasonal cycle is reproduced,
327 likely reflects the coarser resolution of T14 the product than the reconstruction (4°x5°
328 vs. 1°x1°) and the spatial interpolation required to generate T14.

329 As result of this analysis we believe that in the Australian region our reconstruction
330 offers an improved and higher resolution representation of the mean state and
331 seasonality than T14. This comparison also underscores the need for such ongoing
332 regional analyses, and the limitations of using large-scale global products such as T14
333 to understand regional variability and change.

334

335 **4.5 Historical Changes**

336 Historical change in ocean acidification since 1870 is represented in Figure 7 by the
337 changes in the mean annual values of pH and aragonite saturation state between the
338 period 1870-1889 and 1990-2009 (Figure 7). The corresponding changes in sea
339 surface temperature (HadiSST; Rayner et al., 2003) are shown over the same period,
340 indicating a small net warming of the waters around Australia. This warming has
341 been relatively uniform with the exception of the northern edge of the Southern
342 Ocean, and Southeastern Australia which is identified as a marine hotspot by Hobday
343 and Pecl (2013). The ocean acidification changes due to ocean carbon uptake driven
344 by increasing atmospheric CO2, rather than changes in SST. The changes with time in
345 pH and saturation state at the IMOS-NRS sites are plotted in Figure 9.

346 Our reconstruction shows the oceanic carbon uptake over the last 120 years has

resulted in a (spatial) mean decrease in aragonite saturation state of 0.49. As illustrated in Figure 9 these decreases are not constant with time and the change in aragonite saturation state is accelerating. There is also a strong latitudinal gradient in magnitude of the decrease, with larger changes occurring in Northern Australian waters and smaller changes to the south. However the largest decreases in aragonite saturation state (>0.6) have occurred in the Tasman Sea and along the southern coast of Australia. These large changes are illustrated at the NRS sites Port Hacking, Ningaloo and Kangaroo Island (Figure 10). This pattern of change around Australia is consistent with large-scale chemical buffering capacity of the ocean (Revelle factor) which increases from ~ 9 at the equator to >11 at bottom of the study region e.g. Sabine et al. (2004).

Consistent with aragonite saturation state over the last 120 years there has been a net decease in pH of 0.09 units, very close to the estimated global decrease of 0.1 pH by (Caldeira and Wickett, 2003) over a similar period. Consistent with aragonite saturation a strong latitudinal gradient in pH is evident, but it is the inverse. The largest changes in pH have occurred in Southern Australia e.g. Maria Island (Figure 9), with the smallest changes in Northern Australian waters (e.g. Yongala (Figure 9) is about 75% of the change experienced in the south). This spatial response of pH is primarily set by the gradient of ocean mean temperature that acts to increase pH in colder waters (Figure 8).

4.6 Interannual Variability

Our reconstruction simulates the magnitude of interannual variability around Australia (Figure 7) in pH and aragonite saturation state over the period 1870-2013. The magnitude of the interannual variability at the 2-σ level was also calculated after the long-term trend in aragonite saturation state and pH were removed using a 20-year running mean filter (Figure 9).

We see that the magnitude of the interannual variability in aragonite saturation state from the reconstruction is small (0.05 domain averaged; 2-σ) and spatially quite heterogeneous; with the largest interannual variability in aragonite saturation state occurring in the far eastern Tasman Sea associated with the largest interannual

variability in SST. In contrast the smallest variability is seen along the boundary of the Southern Ocean where SST interannual variability is least. Consistent with aragonite saturation state the pH interannual variability is small (0.002 domain averaged; 2-σ) around Australia. While there appears to be more spatial heterogeneity in the response of pH, the magnitude is very small. Nevertheless, we do see areas of concomitant variability in pH and aragonite saturation state suggesting that in these regions there is interannual variability in the supply of carbon and nutrients to the surface ocean, which in turn would alter the chemistry of the surface waters rather than SST changes alone.

To put the interannual variability in aragonite saturation state and pH in context we calculate the ratio of seasonal variability to interannual variability in Figure 10. The dominant scale of variability is seasonal for both aragonite saturation state and pH, however there is a distinct spatial pattern to this ratio (Figure 10). For aragonite saturation state, the seasonal variability is larger than interannual variability in the South, while the ratio of seasonal variability is much closer to the magnitude of interannual variability in the Coral Sea. This means that observationally separating seasonal changes from interannual changes will be challenging, and may have implications for interpreting observational records. By contrast, around most of Australia the seasonal variability in pH dominates interannual variability with the exception of the Tasman Sea and is much larger than the ratio for aragonite saturation state. In the Tasman Sea, the magnitude of the seasonal variability is close to unity suggesting that in this region it would again be difficult to separate seasonal changes from interannual changes.

4.7 Robustness of the reconstruction

The interannual variability and trend in aragonite saturation state and pH in the reconstruction as presented are driven wholly by SST and atmospheric CO_2, and thereby neglects any changes in interannual variability due to changes in salinity and biological production. Observationally, studies have suggested that in some regions around Australia changes in salinity over the last 50 years have occurred e.g. Durack and Wijffels (2010), while other regions have remained constant over the last 200

409 years e.g. Calvo et al. (2007). If we assume, consistent with (Durack et al., 2012), that
410 the changes are related to evaporation – precipitation (E-P) rather than local riverine
411 input which can have large local inputs of DIC, ALK and potentially nutrients
412 (Hieronymus and Walin, 2013), then any increase in salinity can be treated as
413 freshwater input only . Consequently given the small trends, relative to the mean, and
414 the very low sensitivity of oceanic pCO_2 to freshwater input (< 1%), it is highly
415 unlikely that such changes would make such a significant difference on pH or
416 aragonite over the last 50 years. This is perhaps not surprising given that freshwater
417 water changes are a dilution flux acting equally on DIC and total alkalinity (Lenton et
418 al., 2012).
419 The nutrients driving variability in ocean acidification are also not considered in this
420 study, as we assume that nutrients are zero around Australia. While this is not strictly
421 true, most waters around Australia are oligotrophic in nature (Condie and Dunn,
422 2006). If the climatological values of silicate and nitrate from CARS (Ridgway et al.,
423 2002) are used to calculate carbonate chemistry, we find only a small bias (0.0007 in
424 aragonite saturation state and 0.005 in pH) in our reconstruction. While we would like
425 to have used a time-evolving field, analogous to salinity, at present no long-term time
426 series are available to use in this reconstruction.

427 In this study we assumed that the seasonal air-sea disequilibrium (ΔpCO_2) is
428 seasonally time invariant i.e. no interannual variability, in the absence of longer-term
429 observational datasets of oceanic pCO_2. At present products the existing products of
430 oceanic pCO_2 fields that do exist e.g. (Landschützer et al., 2014) typically only extend
431 back in time several decades reflecting the limit of historical observations.
432 Consequently these products can not be used to reconstruct long-term changes in
433 ocean acidification.

434 In reality oceanic pCO_2 will be impacted by changes in ocean dynamics and
435 biological production. As primary production is very low around much of Australia
436 (Condie and Dunn, 2006) (<0.2 mgm^{-3}) it is unlikely that even a doubling of primary
437 productivity in response to changes in nutrient supply could induce large changes in
438 oceanic pCO_2 around Australia. Consequently it is unlikely that variability in primary
439 production plays a large role in modulating oceanic pCO_2 levels. In response to
440 changes in circulation only the variability in SST in the carbonate chemistry is

441 accounted for in our reconstruction. While this variability maybe important at shorter-
442 term timescales e.g. Sitch et al (2015) it is still not clear how important these changes
443 are at decadal and longer timescales (Fay and McKinley, 2013). This highlights the
444 need for products based on sustained long-term observations to better understand and
445 characterize variability and change in ocean acidification.

446 **5. Conclusion**

447 To explore how Australia's marine environment has changed, we have synthesized
448 newly acquired in situ observations of carbon chemistry around Australia to: (i)
449 provide an new estimate of the mean state of pH and aragonite saturation state, (ii)
450 estimate seasonal and interannual variability since 1870; and (iii) reconstruct the
451 changes in ocean acidification around Australia since 1870.

452 In this work we developed a new alkalinity-salinity relationship for the Australian
453 region. This relationship was used in conjunction with observed salinity and oceanic
454 and atmospheric CO_2 and SST data, to reconstruct the present and past changes in pH
455 and aragonite saturation state. Our reconstructed fields were compared against the
456 Takahashi et al (2014) climatology and high-resolution data collected at the IMOS-
457 NRS sites. We found good agreement between our reconstructed fields for the
458 observed annual mean and seasonal cycles at the shelf IMOS-NRS sites except
459 regions such as the Great Barrier Reef where nearshore processes and coral reef
460 metabolism could alter the pH and saturation state.

461 Our regional reconstruction provides much higher spatial and temporal resolution than
462 previous global estimates. This highlights the importance of regional analysis and
463 reconstructions in estimating and understanding region changes. An important result
464 of this study is that at present the Coral Sea is not experiencing marginal conditions
465 (values of aragonite saturation state < 3.5) with respect to ocean acidification as has
466 been suggested.

467 Large changes in aragonite saturation state and pH have occurred over the last 140
468 years in response to increasing oceanic uptake of atmospheric CO_2. A net (spatial)
469 mean decrease in pH of 0.09 is seen in the period (1990-2009) – (1889-1870),
470 together with a net decrease in aragonite saturation state of 0.49, both of which are
471 consistent with previous estimates of the historical trends. Importantly, due to ocean

chemistry, the spatial pattern of the change in aragonite saturation state and pH are different. In this study we found the largest changes in aragonite saturation state occurred at mid and low latitudes, and the largest changes in pH occurred at higher latitudes.

The large seasonal variability around Australia is heterogeneous, with distinctly different spatial patterns in aragonite saturation state and pH apart from South of Australia where variability is driven by deep winter mixing. For aragonite saturation state, large seasonal variability occurs off the East Coast of Australia and in Tasman Sea driven by seasonal variability in ocean temperatures. Generally, the magnitude of seasonal variability exceeds IAV in the Australian region with the exception of pH in Tasman Sea, and aragonite saturation state in the tropical ocean. In these regions the magnitude of interannual variability is comparable to seasonal variability, which has potential implications for interpreting observed biological changes over different timescales.

The variability in aragonite saturation state and pH are spatially different over regional scales and all time scales, implying that biological responses and impacts are likely vary. Further, this suggests that both pH and aragonite (or calcite) saturation state need to be considered independently in assessing ecosystem responses and changes.

The goal of this historical reconstruction also provides useful information to link with biological observations to help understand observed changes and aid in the design of future work, thereby elucidating the consequences of Ocean Acidification. To facilitate this all of the reconstructed data is available at http://imos.aodn.org.au

6. Acknowledgments

AL, BT and RJM acknowledge support from the Australian Climate Change Science Program. TPS would like to acknowledge funding support for the CSIRO carbon cluster. YN was supported by JSPS KAKENHI Grant Number 26220102. The authors would like to thank the Integrated Marine Observing System (IMOS) for providing data from the Australian National Research Sites (NRSs), and Kate Berry and Kristina Patterson for their analysis of the observed carbon data.

7. References

Albright, R., Langdon, C., and Anthony, K. R. N.: Dynamics of seawater carbonate chemistry, production, and calcification of a coral reef flat, Central Great Barrier Reef, Biogeosciences, 10, 6747-6758, 2013.

Antonov, J. I., Seidov, D., Boyer, T. P., Locarnini, R. A., Mishonov, A. V., Garcia, H. E., Baranova, O. K., Zweng, M. M., and Johnson, D. R., World Ocean Atlas 2009, Volume 2: Salinity, in, edited by: Levitus, S., NOAA Atlas NESDIS 69, U.S. Government Printing Office, Washington, D.C., 184 pp, 2010

Bell, J. D., JE, J., and AJ, H.: Vulnerability of Tropical Pacific Fisheries and Aquaculture to Climate Change, Secretariat of the Pacific Community, Noumea, New Caledonia, 2011.

Caldeira, K., and Wickett, M. E.: Anthropogenic carbon and ocean pH, Nature, 425, 365-365, Doi 10.1038/425365a, 2003.

Calvo, E., Marshall, J. F., Pelejero, C., McCulloch, M. T., Gagan, M. K., and Lough, J. M.: Interdecadal climate variability in the Coral Sea since 1708 AD, Palaeogeogr Palaeocl, 248, 190-201, Doi 10.1016/J.Palaeo.2006.12.003, 2007.

Ciais, P., Sabine, C., Bala, G., Bopp, L., Brovkin, V., Canadell, J., Chhabra, A., Defriers, R., Galloway, J. N., Heinman, M., Jones, C. D., Le Quéré, C., Myneni, R. B., Piao, S., and Thornton, P.: Carbon and Other Biogeochemical Cycles, in: Climate Change 2013: The Physical Science Basis. Contribution of Working Group I to the Fifth Assessment Report of the Intergovernmental Panel on Climate Change edited by: Stocker, T. F., Qin, D., Plattner, G.-K., Tignor, M., Allen, S. K., Boschung, A., A, N., Xia, Y., V., B., and Midgley, P. M., Cambridge University Press, Cambridge, United Kingdom and New York 2013.

Condie, S. A., and Dunn, J. R.: Seasonal characteristics of the surface mixed layer in the Australasian region: implications for primary production regimes and biogeography, Marine and Freshwater Research, 57, 569-590, Doi 10.1071/Mf06009_Lr, 2006.

Dickson, A. G., and F. J. Millero, A comparison of the equilibrium constants for the dissociation of carbonic acid in seawater media, Deep Sea Res., Part I, 34, 1733–1743, doi:10.1016/0198-0149(87)90021-5, 1987

Doney, S. C., Balch, W. M., Fabry, V. J., and Feely, R. A.: Ocean Acidification: A Critical Emerging Problem for the Ocean Sciences, Oceanography, 22, 16-+, Doi 10.5670/Oceanog.2009.93, 2009.

Doney, S. C., Ruckelshaus, M., Duffy, J. E., Barry, J. P., Chan, F., English, C. A., Galindo, H. M., Grebmeier, J. M., Hollowed, A. B., Knowlton, N., Polovina, J., Rabalais, N. N., Sydeman, W. J., and Talley, L. D.: Climate Change Impacts on Marine Ecosystems, Annu Rev Mar Sci, 4, 11-37, Doi 10.1146/Annurev-Marine-041911-111611, 2012.

537 Dore, J. E., Lukas, R., Sadler, D. W., Church, M. J., and Karl, D. M.: Physical and
538 biogeochemical modulation of ocean acidification in the central North Pacific, P Natl Acad
539 Sci USA, 106, 12235-12240, Doi 10.1073/Pnas.0906044106, 2009.
540 Durack, P. J., and Wijffels, S. E.: Fifty-Year Trends in Global Ocean Salinities and Their
541 Relationship to Broad-Scale Warming, Journal of Climate, 23, 4342-4362, Doi
542 10.1175/2010jcli3377.1, 2010.
543 Durack, P. J., Wijffels, S. E., and Matear, R. J.: Ocean Salinities Reveal Strong Global Water
544 Cycle Intensification During 1950 to 2000, Science, 336, 455-458, Doi
545 10.1126/Science.1212222, 2012.
546 Fabricius, K. E., Langdon, C., Uthicke, S., Humphrey, C., Noonan, S., De'ath, G., Okazaki,
547 R., Muehllehner, N., Glas, M. S., and Lough, J. M.: Losers and winners in coral reefs
548 acclimatized to elevated carbon dioxide concentrations, Nat Clim Change, 1, 165-169, Doi
549 10.1038/Nclimate1122, 2011.
550 Fabry, V. J., Seibel, B. A., Feely, R. A., and Orr, J. C.: Impacts of ocean acidification on
551 marine fauna and ecosystem processes, Ices J Mar Sci, 65, 414-432, Doi
552 10.1093/Icesjms/Fsn048, 2008.
553 Fay, A. R., and G. A. McKinley, Global trends in surface ocean pCO_2 from in situ data,
554 Global Biogeochem. Cycles, 27, 541–557, doi:10.1002/gbc.20051, 2013

555 Frolicher, T. L., and Joos, F.: Reversible and irreversible impacts of greenhouse gas emissions
556 in multi-century projections with the NCAR global coupled carbon cycle-climate model, Clim
557 Dynam, 35, 1439-1459, Doi 10.1007/S00382-009-0727-0, 2010.
558 Gagliano, M., McCormick, M. I., Moore, J. A., and Depczynski, M.: The basics of
559 acidification: baseline variability of pH on Australian coral reefs, Marine Biology, 157, 1849-
560 1856, Doi 10.1007/S00227-010-1456-Y, 2010.
561 Garcia, H. E., Locarnini, R. A., Boyer, T. P., Antonov, J. I., Baranova, O. K., Zweng, M. M.,
562 and Johnson, D. R. (2010a), World Ocean Atlas 2009, Volume 3: Dissolved Oxygen
563 Apparent Oxygen Utilization, and Oxygen Saturation, in, edited by: Levitus, S., NOAA Atlas
564 NESDIS 70, U.S. Government Printing Office, Washington, D.C., 344 pp.
565 Garcia, H. E., Locarnini, R. A., Boyer, T. P., Antonov, J. I., Zweng, M. M., Baranova, O. K.,
566 and Johnson, D. R., World Ocean Atlas 2009, Volume 4: Nutrients (phosphate, nitrate,
567 silicate), in, edited by: Levitus, S., NOAA Atlas NESDIS 71, U.S. Government Printing
568 Office, Washington, D.C., 398 pp., 2010b
569 Garcia, H. E., Locarnini, R. A., Boyer, T. P., Antonov, J. I., Baranova, O. K., Zweng, M. M.,
570 Reagan, J. R., and Johnson, D. R., World Ocean Atlas 2013, Volume 3: Dissolved Oxygen,
571 Apparent Oxygen Utilization, and Oxygen Saturation, in, edited by: Levitus, S., and
572 Mishonov, A., NOAA Atlas NESDIS 75, 27 pp, 2014a

Garcia, H. E., Locarnini, R. A., Boyer, T. P., Antonov, J. I., Baranova, O. K., Zweng, M. M., Reagan, J. R., and Johnson, D. R., World Ocean Atlas 2013, Volume 4: Dissolved Inorganic Nutrients (phosphate, nitrate, silicate), in, edited by: Levitus, S., and Mishonov, A., NOAA Atlas NESDIS 76, 25, 25 pp., 2014b

Guinotte, J. M., Buddemeier, R. W., and Kleypas, J. A.: Future coral reef habitat marginality: temporal and spatial effects of climate change in the Pacific basin, Coral Reefs, 22, 551-558, Doi 10.1007/S00338-003-0331-4, 2003.

Hauck, J., and C. Völker, Rising atmospheric CO_2 leads to large impact of biology on Southern Ocean CO2 uptake via changes of the Revelle factor, Geophys. Res. Lett., 42, 1459–1464, doi:10.1002/2015GL063070, 2015

Hieronymus, J., and Walin, G.: Unravelling the land source: an investigation of the processes contributing to the oceanic input of DIC and alkalinity, Tellus B, 65, Artn 19683 Doi 10.3402/Tellusb.V65i0.19683, 2013.

Hobday, A. J., and Pecl, G. T.: Identification of global marine hotspots: sentinels for change and vanguards for adaptation action, Rev Fish Biol Fisheries, 10.1007/s11160-013-9326-6, 2013.

Iglesias-Rodriguez, M. D., Halloran, P. R., Rickaby, R. E. M., Hall, I. R., Colmenero-Hidalgo, E., Gittins, J. R., Green, D. R. H., Tyrrell, T., Gibbs, S. J., von Dassow, P., Rehm, E., Armbrust, E. V., and Boessenkool, K. P.: Phytoplankton calcification in a high-CO2 world, Science, 320, 336-340, Doi 10.1126/Science.1154122, 2008.

Key, R. M., Kozyr, A., Sabine, C. L., Lee, K., Wanninkhof, R., Bullister, J. L., Feely, R. A., Millero, F. J., Mordy, C., and Peng, T. H.: A global ocean carbon climatology: Results from Global Data Analysis Project (GLODAP), Global Biogeochemical Cycles, 18, Artn Gb4031 Doi 10.1029/2004gb002247, 2004.

Kuchinke, M., Tilbrook, B., and Lenton, A.: Seasonal variability of aragonite saturation state in the Western Pacific, Mar Chem, 161, 1-13, Doi 10.1016/J.Marchem.2014.01.001, 2014.

Langdon, C.: Effect of elevated pCO2 on photosynthesis and calcification of corals and interactions with seasonal change in temperature/irradiance and nutrient enrichment, Journal of Geophysical Research, 110, 10.1029/2004jc002576, 2005.

Le Quéré, C., Moriarty, R., Andrew, R. M., Peters, G. P., Ciais, P., Friedlingstein, P., Jones, S. D., Sitch, S., Tans, P., Arneth, A., Boden, T. A., Bopp, L., Bozec, Y., Canadell, J. G., Chini, L. P., Chevallier, F., Cosca, C. E., Harris, I., Hoppema, M., Houghton, R. A., House, J. I., Jain, A. K., Johannessen, T., Kato, E., Keeling, R. F., Kitidis, V., Klein Goldewijk, K., Koven, C., Landa, C. S., Landschützer, P., Lenton, A., Lima, I. D., Marland, G., Mathis, J. T., Metzl, N., Nojiri, Y., Olsen, A., Ono, T., Peng, S., Peters, W., Pfeil, B., Poulter, B., Raupach,

609 M. R., Regnier, P., Rödenbeck, C., Saito, S., Salisbury, J. E., Schuster, U., Schwinger, J.,
610 Séférian, R., Segschneider, J., Steinhoff, T., Stocker, B. D., Sutton, A. J., Takahashi, T.,
611 Tilbrook, B., van der Werf, G. R., Viovy, N., Wang, Y. P., Wanninkhof, R., Wiltshire, A.,
612 and Zeng, N.: Global carbon budget 2014, 7, 47-85, doi:10.5194/essd-7-47-2015, 2015.
613 Lee, K., Tong, L. T., Millero, F. J., Sabine, C. L., Dickson, A. G., Goyet, C., Park, G. H.,
614 Wanninkhof, R., Feely, R. A., and Key, R. M.: Global relationships of total alkalinity with
615 salinity and temperature in surface waters of the world's oceans, Geophys Res Lett, 33, -, Artn
616 L19605 Doi 10.1029/2006gl027207, 2006.
617 Lenton, A., Metzl, N., Takahashi, T., Kuchinke, M., Matear, R. J., Roy, T., Sutherland, S. C.,
618 Sweeney, C., and Tilbrook, B.: The observed evolution of oceanic pCO(2) and its drivers over
619 the last two decades, Global Biogeochemical Cycles, 26, Artn Gb2021, Doi
620 10.1029/2011gb004095, 2012.
621 Lima, F. P., and Wethey, D. S.: Three decades of high-resolution coastal sea surface
622 temperatures reveal more than warming, Nat Commun, 3, Artn 704
623 Doi 10.1038/Ncomms1713, 2012.
624 Locarnini, R. A., Mishonov, A. V., Antonov, J. I., Boyer, T. P., Garcia, H. E., Baranova, O.
625 K., Zweng, M. M., and Johnson, D. R, World Ocean Atlas 2009, Volume 1: Temperature, in,
626 edited by: Levitus, S., Ed. NOAA Atlas NESDIS 68, U.S. Government Printing Office,
627 Washington, D.C., 184 pp., 2010
628 Locarnini, R. A., Mishonov, A. V., Antonov, J. I., Boyer, T. P., Garcia, H. E., Baranova, O.
629 K., Zweng, M. M., Paver, C. R., Reagan, J. R., Johnson, D. R., Hamilton, M., and Seidov, D.
630 World Ocean Atlas 2013, Volume 1: Temperature, in, edited by: S. Levitus, E., and A.
631 Mishonov, T. E., NOAA Atlas NESDIS 73, 40 pp, 2013
632 Lynch, T. P., Morello, E. B., Evans, K., Richardson, A., Rochester, J. W. C., Steinberg, C. R.,
633 Roughan, M., Thompson, P., Middleton, J. F., Feng, M., Sherrington, R., Brando, V.,
634 Tilbrook, B., Ridgway, K., Allen, S., Doherty, P., Hill, K., and Moltmann, T. C.: IMOS
635 National Reference Stations: a continental wide physical, chemical and biological coastal
636 observing system. , PLOS One, 9(12): e113652, doi:10.1371/journal.pone.0113652, 2014.
637 Matear, R. J., and Lenton, A.: Quantifying the impact of ocean acidification on our future
638 climate, Biogeosciences, 11, 3965-3983, doi: 10.5194/Bg-11-3965-2014, 2014.
639 Mehrbach, C., C. H. Culberson, J. E. Hawley, and R. M. Pytkowicz, Measurement of the
640 apparent dissociation constants of carbonic acid in seawater at atmospheric pressure, Limnol.
641 Oceanogr., 18, 897–907,doi:10.4319/lo.1973.18.6.0897, 1973.
642 Mucci, A.: The Solubility of Calcite and Aragonite in Seawater at Various Salinities,
643 Temperatures, and One Atmosphere Total Pressure, Am J Sci, 283, 780-799, 1983.

644 Munday, P. L., Donelson, J. M., Dixson, D. L., and Endo, G. G. K.: Effects of ocean
645 acidification on the early life history of a tropical marine fish, P Roy Soc B-Biol Sci, 276,
646 3275-3283, Doi 10.1098/Rspb.2009.0784, 2009.
647 Munday, P. L., Dixson, D. L., McCormick, M. I., Meekan, M., Ferrari, M. C. O., and Chivers,
648 D. P.: Replenishment of fish populations is threatened by ocean acidification, P Natl Acad Sci
649 USA, 107, 12930-12934, doi:10.1073/Pnas.1004519107, 2010.
650 Pelejero, C., Calvo, E., McCulloch, M. T., Marshall, J. F., Gagan, M. K., Lough, J. M., and
651 Opdyke, B. N.: Preindustrial to modern interdecadal variability in coral reef pH, Science, 309,
652 2204-2207, Doi 10.1126/Science.1113692, 2005.
653 Rayner, N. A., Parker, D. E., Horton, E. B., Folland, C. K., Alexander, L. V., Rowell, D. P.,
654 Kent, E. C., and Kaplan, A.: Global analyses of sea surface temperature, sea ice, and night
655 marine air temperature since the late nineteenth century, J Geophys Res-Atmos, 108, Artn
656 4407,doi:10.1029/2002jd002670, 2003.
657 Reynolds, R. W., Smith, T. M., Liu, C., Chelton, D. B., Casey, K. S., and Schlax, M. G.:
658 Daily high-resolution-blended analyses for sea surface temperature, Journal of Climate, 20,
659 5473-5496, Doi 10.1175/2007jcli1824.1, 2007.
660 Ricke, K. L., Orr, J. C., Schneider, K., and Caldeira, K.: Risks to coral reefs from ocean
661 carbonate chemistry changes in recent earth system model projections, Environ Res Lett, 8,
662 Artn 034003, Doi 10.1088/1748-9326/8/3/034003, 2013.
663 Ridgway, K. R., Dunn, J. R., and Wilkin, J. L.: Ocean interpolation by four-dimensional
664 weighted least squares - application to the waters around Australasia, Journal of Atmospheric
665 and Oceanic Technology, 19, 1357-1375, Doi 10.1175/1520-0426, 2002.
666 Riebesell, U., Fabry, V. J., Hansson, L., and Gattuso, J.-P.: Guide to best practices for ocean
667 acidification research and data reporting, Publications Office of the European Union.,
668 Luxembourg, 260, 2010.
669 Sabine, C. L., Feely, R. A., Gruber, N., Key, R. M., Lee, K., Bullister, J. L., Wanninkhof, R.,
670 Wong, C. S., Wallace, D. W. R., Tilbrook, B., Millero, F. J., Peng, T. H., Kozyr, A., Ono, T.,
671 and Rios, A. F.: The oceanic sink for anthropogenic CO2, Science, 305, 367-371, Doi
672 10.1126/Science.1097403, 2004.
673 Sasse, T. P., McNeil, B. I., and Abramowitz, G.: A new constraint on global air-sea CO2
674 fluxes using bottle carbon data, Geophys Res Lett, 40, 1594-1599, Doi 10.1002/Grl.50342,
675 2013.
676 Shaw, E. C., McNeil, B. I., and Tilbrook, B.: Impacts of ocean acidification in naturally
677 variable coral reef flat ecosystems, J Geophys Res-Oceans, 117, Artn C03038, Doi
678 10.1029/2011jc007655, 2012.

679 Silverman, J., Lazar, B., Cao, L., Caldeira, K., and Erez, J.: Coral reefs may start dissolving
680 when atmospheric CO2 doubles, Geophys Res Lett, 36, Artn L05606
681 Doi 10.1029/2008gl036282, 2009.
682 Stanley, S. M., and Hardie, L. A.: Secular oscillations in the carbonate mineralogy of reef-
683 building and sediment-producing organisms driven by tectonically forced shifts in seawater
684 chemistry, Palaeogeogr Palaeocl, 144, 3-19, Doi 10.1016/S0031-0182(98)00109-6, 1998.
685 Takahashi, T., Sutherland, S. C., Wanninkhof, R., Sweeney, C., Feely, R. A., Chipman, D.
686 W., Hales, B., Friederich, G., Chavez, F., Sabine, C., Watson, A., Bakker, D. C. E., Schuster,
687 U., Metzl, N., Yoshikawa-Inoue, H., Ishii, M., Midorikawa, T., Nojiri, Y., Kortzinger, A.,
688 Steinhoff, T., Hoppema, M., Olafsson, J., Arnarson, T. S., Tilbrook, B., Johannessen, T.,
689 Olsen, A., Bellerby, R., Wong, C. S., Delille, B., Bates, N. R., and de Baar, H. J. W.:
690 Climatological mean and decadal change in surface ocean pCO(2), and net sea-air CO2 flux
691 over the global oceans, Deep-Sea Res Pt Ii, 56, 554-577, Doi 10.1016/J.Dsr2.2008.12.009,
692 2009.
693 Sitch, S., Friedlingstein, P., Gruber, N., Jones, S. D., Murray-Tortarolo, G., Ahlström, A.,
694 Doney, S. C., Graven, H., Heinze, C., Huntingford, C., Levis, S., Levy, P. E., Lomas, M.,
695 Poulter, B., Viovy, N., Zaehle, S., Zeng, N., Arneth, A., Bonan, G., Bopp, L., Canadell, J. G.,
696 Chevallier, F., Ciais, P., Ellis, R., Gloor, M., Peylin, P., Piao, S. L., Le Quéré, C., Smith, B.,
697 Zhu, Z., and Myneni, R.: Recent trends and drivers of regional sources and sinks of carbon
698 dioxide, Biogeosciences, 12, 653-679, doi:10.5194/bg-12-653-2015, 2015.
699 Takahashi, T., Sutherland, S. C., Chipman, D. W., Goddard, J. G., Ho, C., Newberger, T.,
700 Sweeney, C., and Munro, D. R.: Climatological distributions of pH, pCO_2, total CO_2,
701 alkalinity, and $CaCO_3$ saturation in the global surface ocean, and temporal changes at selected
702 locations, Mar Chem, 164, 95-125,doi: 10.1016/j.marchem.2014.06.004, 2014.
703 Zeebe, R. E. and Wolf-Gladrow. CO_2 in Seawater: Equilibrium, Kinetics, Isotopes. Elsevier
704 Oceanography Series, 65, pp. 346, Amsterdam, 2001
705 Zweng, M. M., Reagan, J. R., Antonov, J. I., Locarnini, R. A., Mishonov, A. V., Boyer, T. P.,
706 Garcia, H. E., Baranova, O. K., Johnson, D. R., D.Seidov, and Biddle, M. M. (2013), World
707 Ocean Atlas 2013, Volume 2: Salinity, in, edited by: Levitus, S., and Mishonov, A., NOAA
708 Atlas NESDIS 74, 39 pp.
709
710
711

7. Figures and Tables

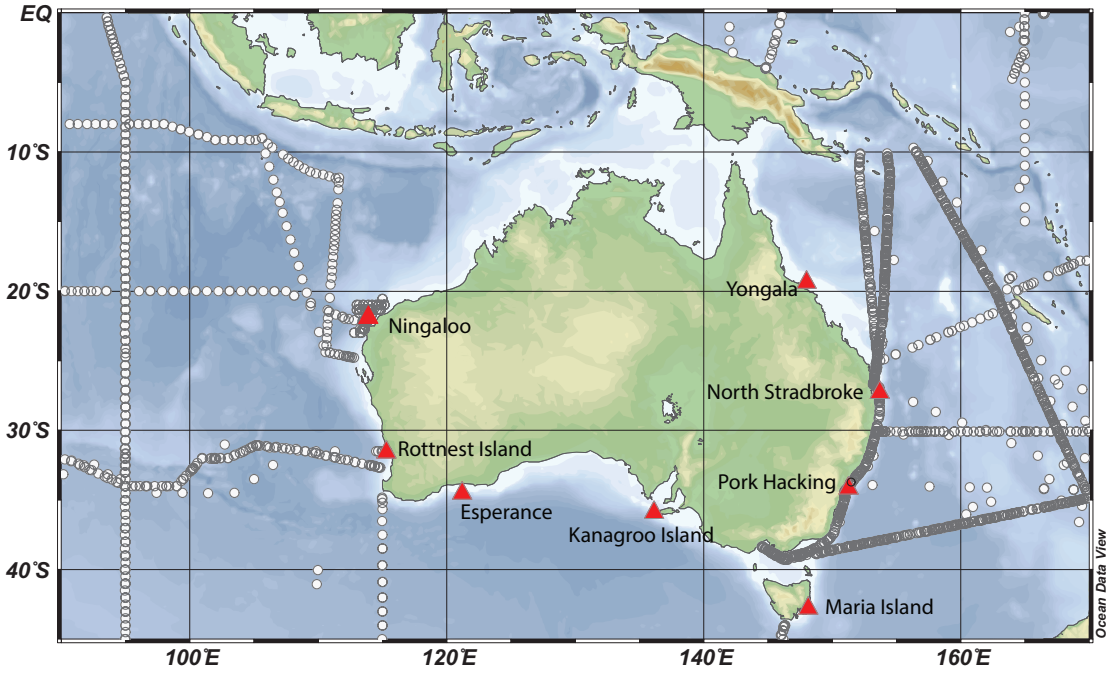

Figure 1 Locations (circles) of the concomitant measurements of alkalinity and salinity used to develop a new salinity-alkalinity relationship for the Australian Region, the cruises are listed in Table 1. Overlain on this plot (red triangles) are the locations of IMOS National Reference Stations (NRS) used in this study.

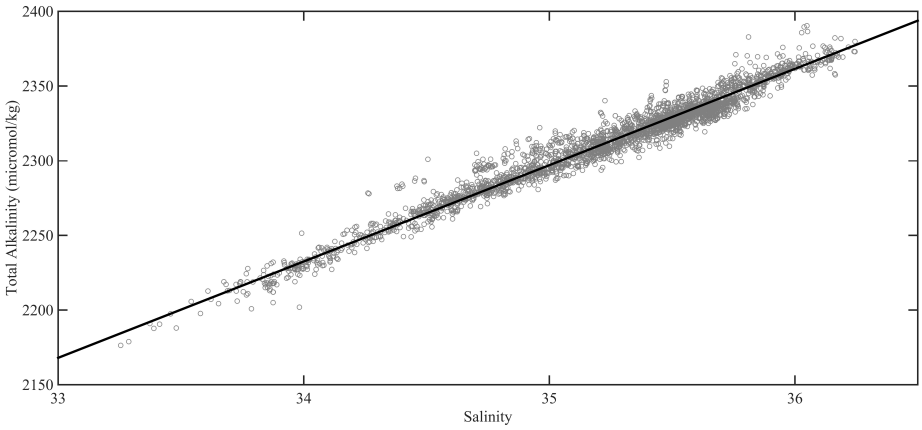

726
727
728 Figure 2 The new salinity-alkalinity relationship developed for the Australian Region
729 based on observations (Figure 1) collected in the period 1992-2011. The individual
730 cruises are listed in Table 1.
731
732
733
734
735
736

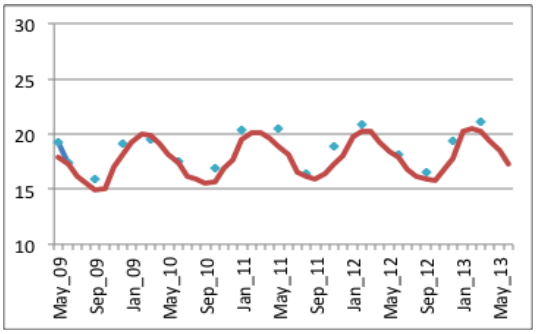

Esperance

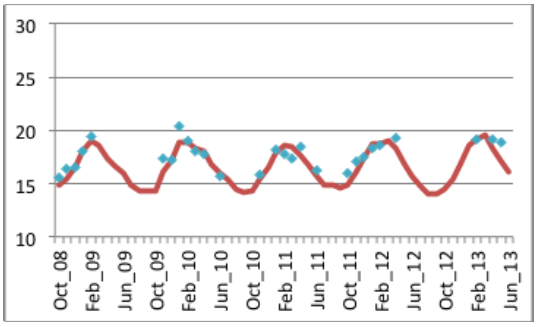

Kangaroo Island

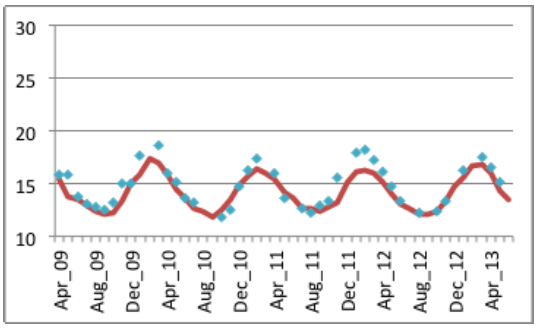

Maria Island

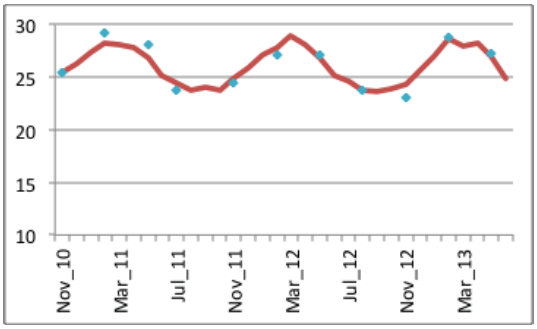

Ningaloo

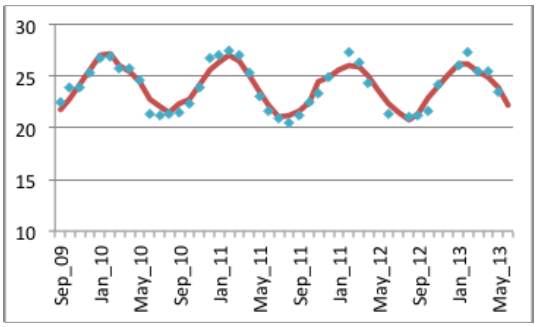

North Stradbroke

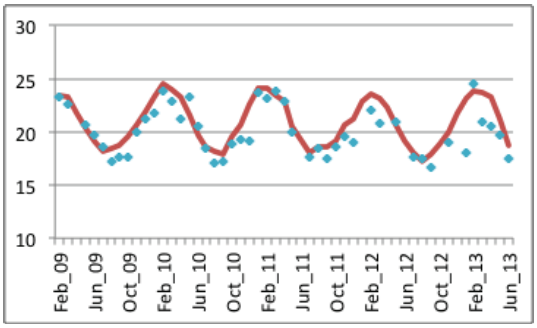

Port Hacking

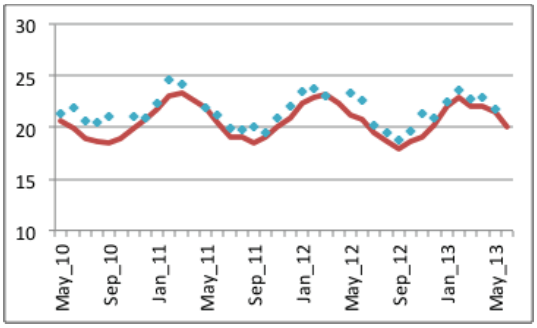

Rottnest

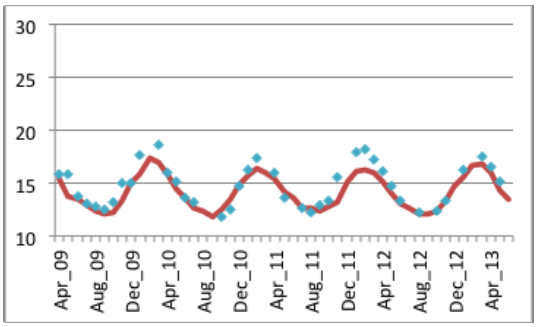

Yongala

Figure 3 Comparison of sea surface temperature from the observations at the IMOS National Research Stations with HadiSST (Rayner et al, 2003)

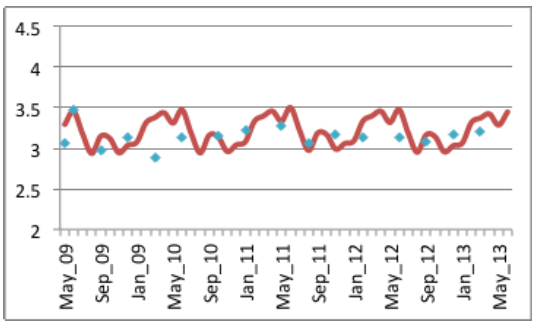

Esperance

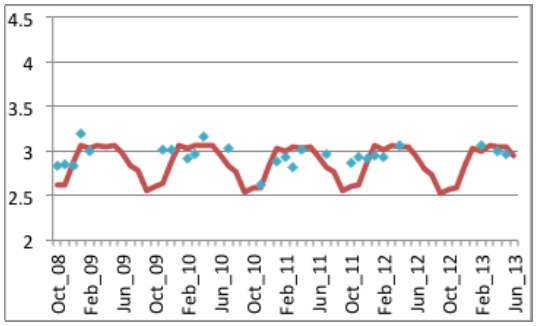

Kangaroo Island

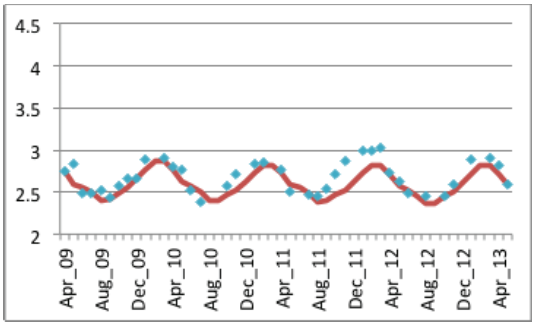

Maria Island

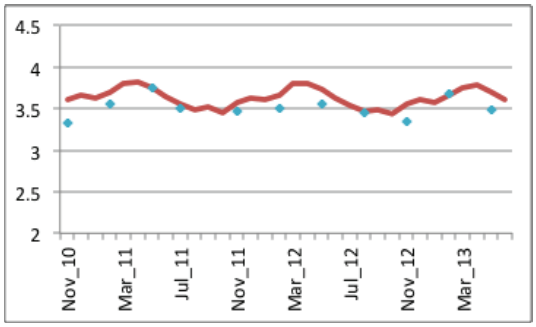

Ningaloo

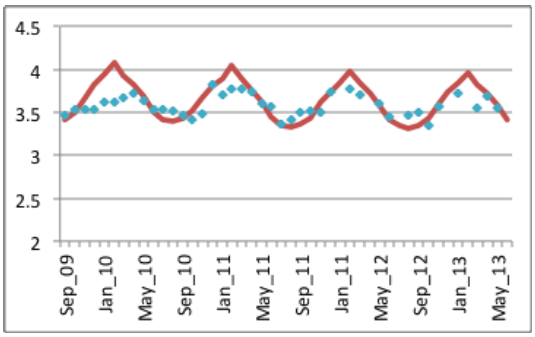

North Stradbroke

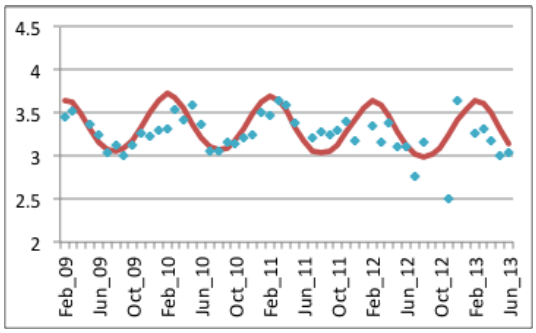

Port Hacking

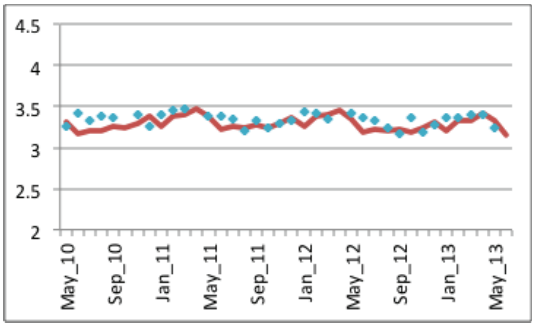

Rottnest

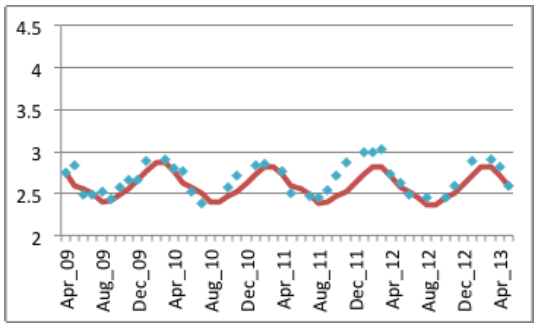

Yongala

Figure 4 Comparison of aragonite saturation state (Ω_{AR}) from the observations at the IMOS National Research Stations with the reconstructed values.

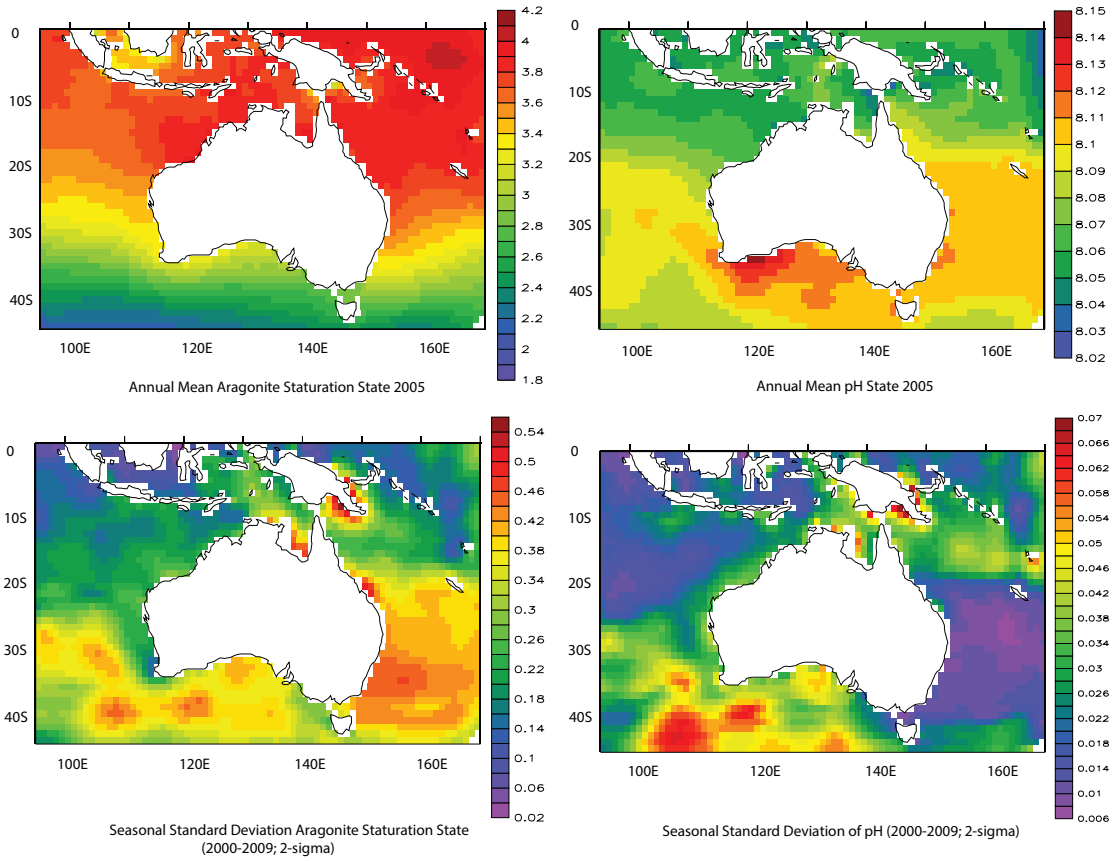

744
745
746

747 Figure 5 Upper: the reconstructed annual mean aragonite saturation state and pH for
748 the period 2000-2009; Lower: the seasonal variability given by 2 times the standard
749 deviation (2-σ) of the seasonal variability in aragonite saturation state and pH from
750 the period 2000-2009.

751

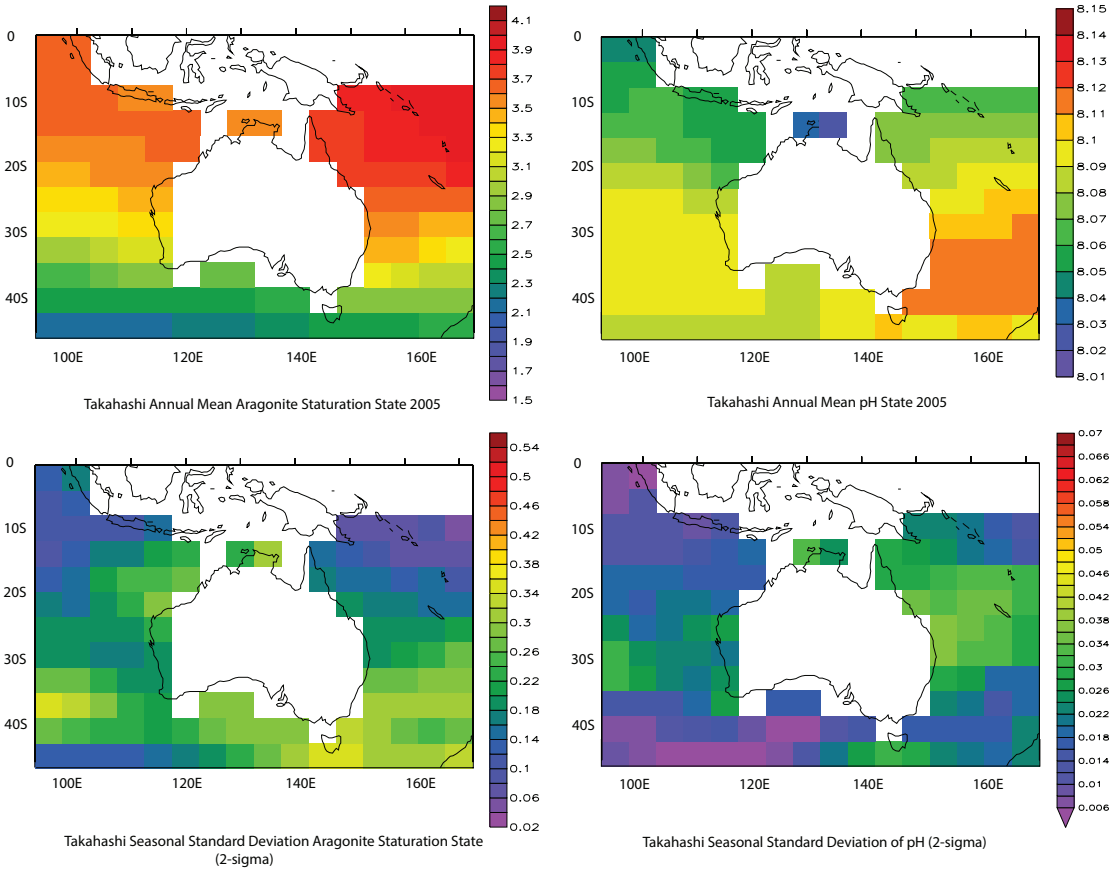

Figure 6 Upper: the annual mean aragonite saturation state and pH for 2005 from Takahashi et al (2014); Lower: standard deviation (2σ) of the seasonal variability in aragonite saturation state and pH for 2005 from Takahashi et al (2014).

.

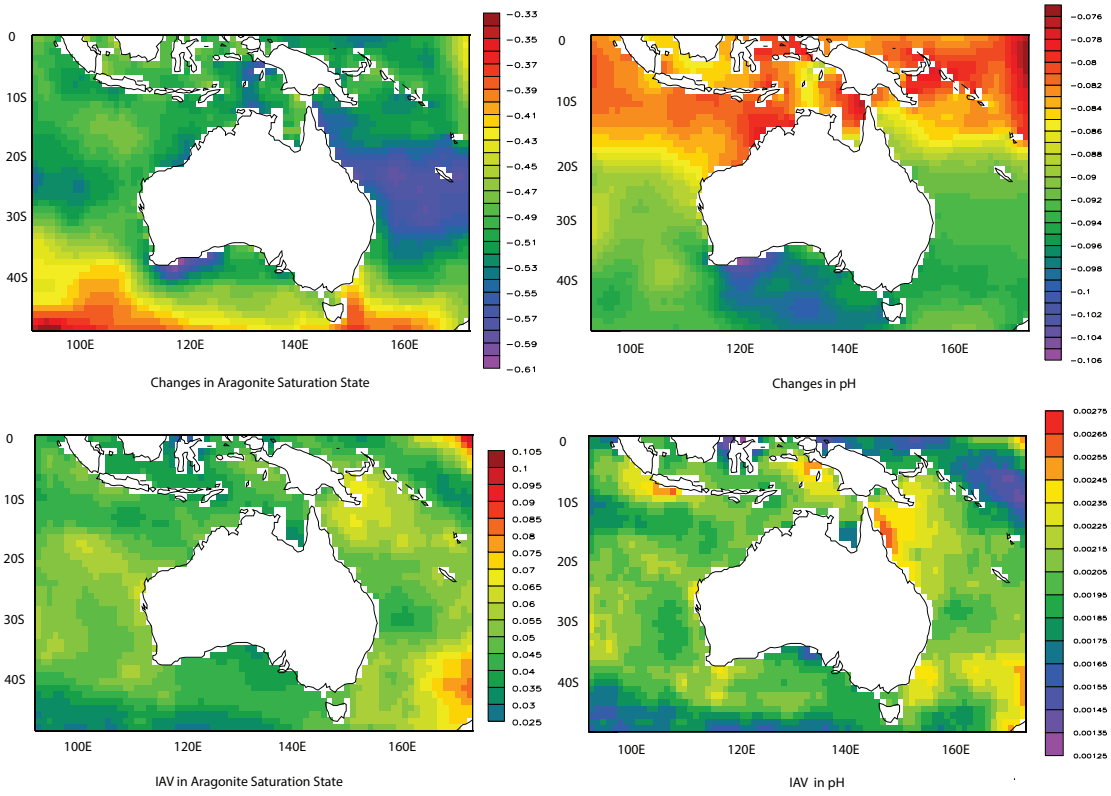

759

760

761 Figure 7 Annual mean 120-year differences (2000-2009 and 1880-1889) in aragonite

762 saturation state and pH (upper); Lower, the interannual variability (IAV) in aragonite

763 saturation state and pH (2σ) over same period

764

765

766

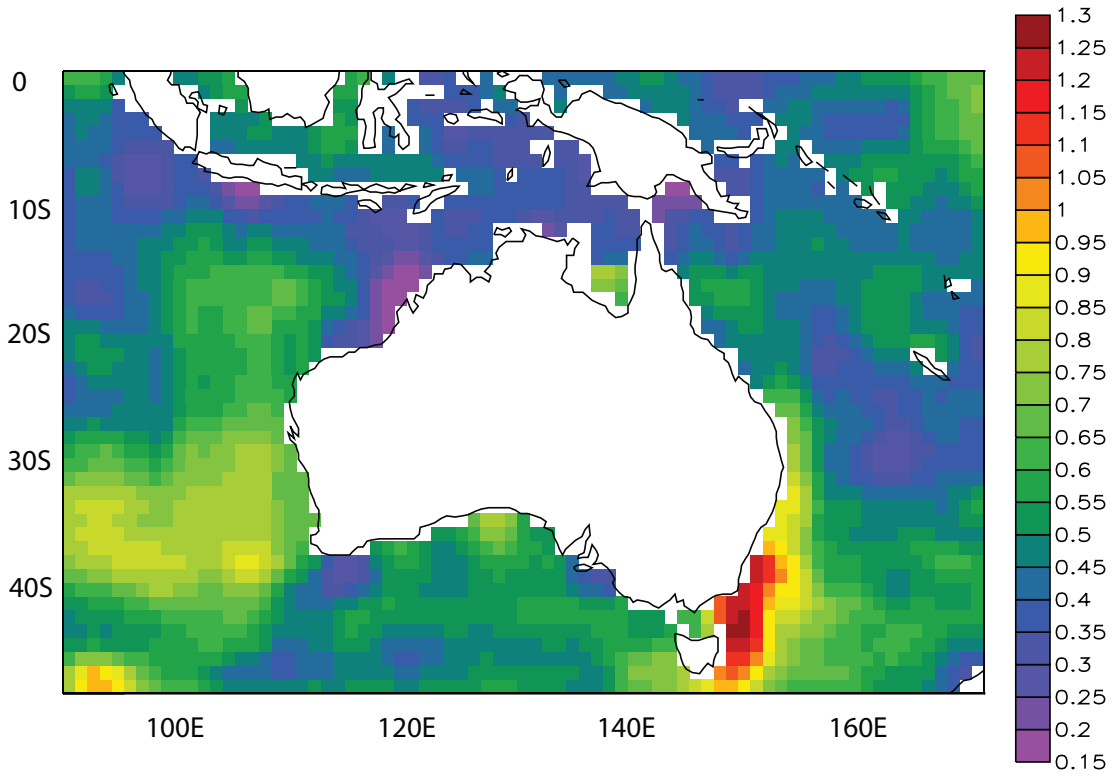

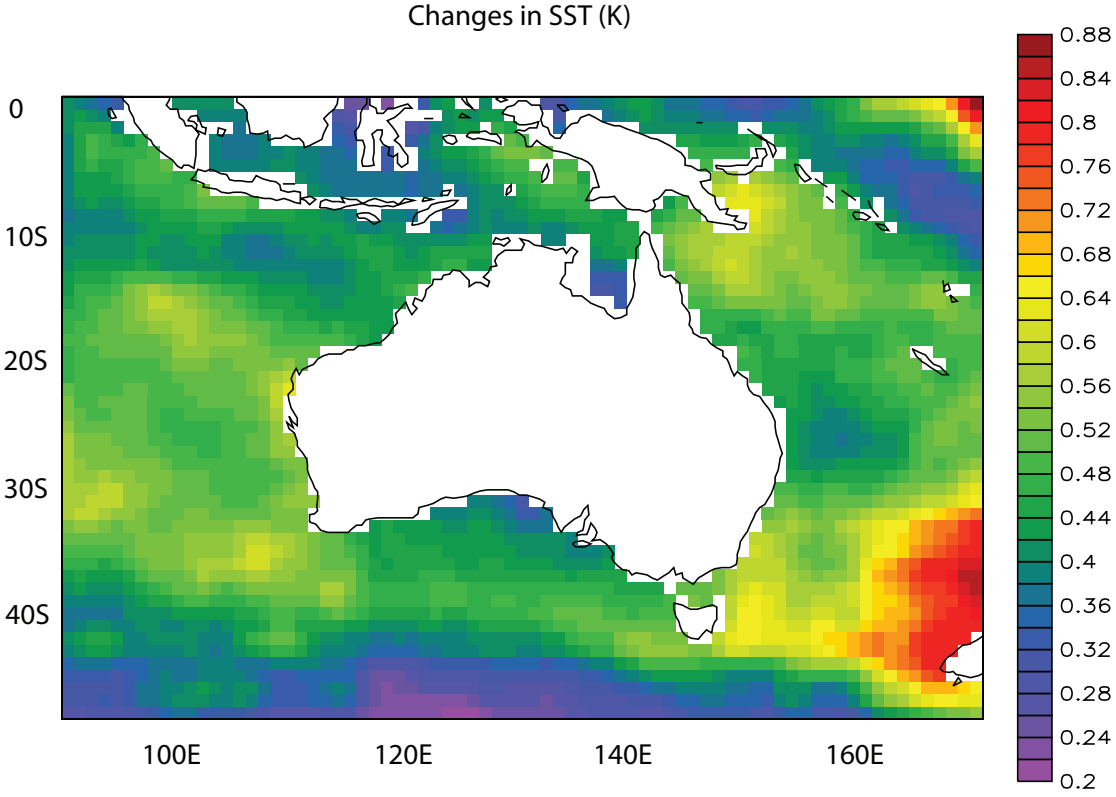

Figure 8 Annual mean 120-year differences (2000-2009 and 1880-1889) in SST (upper); Lower, the interannual variability (IAV) in SST (2σ) over same period. SST data from HadiSST (Rayner et al, 2003).

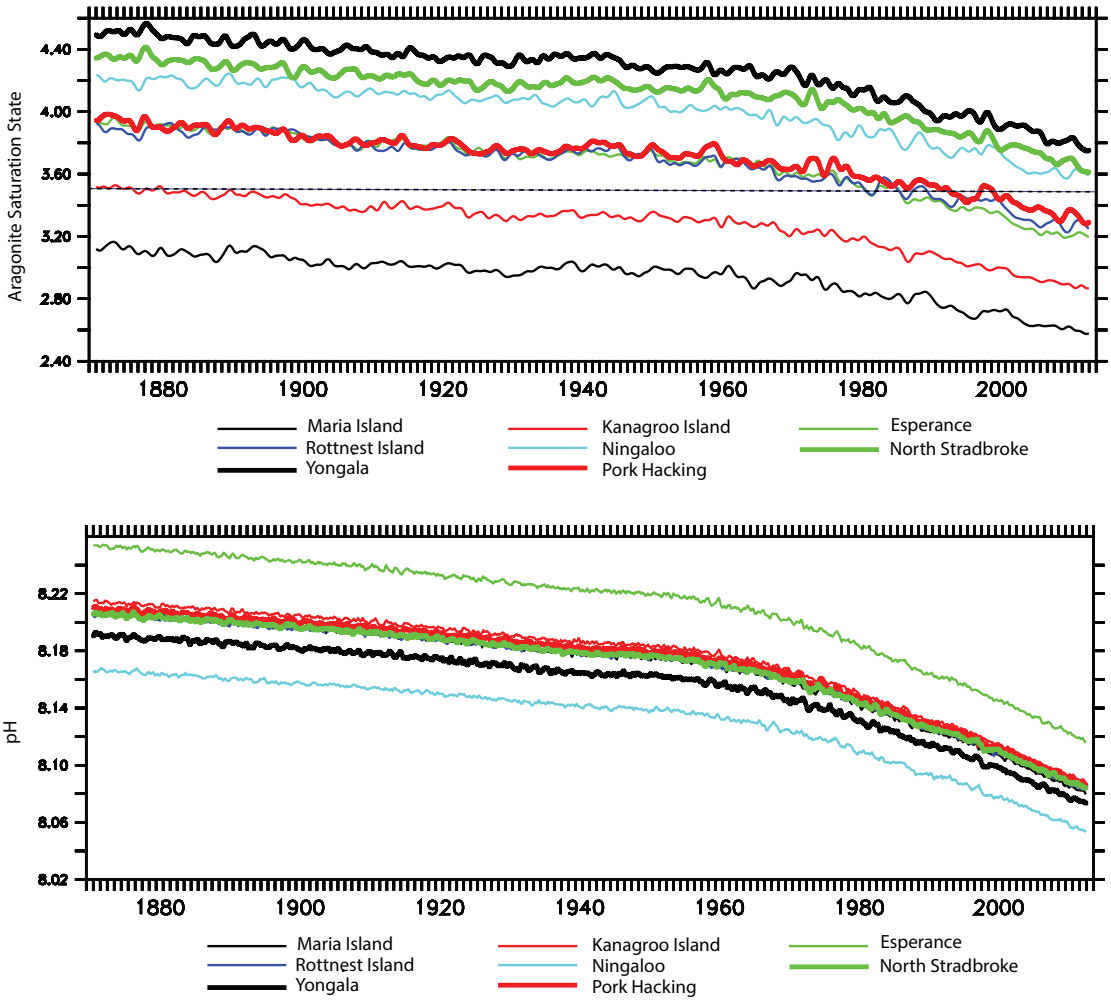

Figure 9 Reconstructed time series of annual mean aragonite saturation state (upper) and pH (lower) at the IMOS-NRSs. Overlain on the upper plot is the threshold for the transition to marginal conditions for coral reefs (3.5) from Guinotte et al. (2003)

Voyage[1]	Region/Expocode	Latitude	Longitude	Period	Number
Section P13	West Pacific 31VIC92_0_1_2	0°S - 5°S	164°E - 165°E	Oct 1992	13
Section P10	West Pacific 3250TN026/1	0°S - 5°S	145°E - 146°E	Oct 1993	11
Section P21	Coral Sea 318M19940327	17°S - 25°S	155°E - 170°E	Jun 1994	49
Section P9	West Pacific 49RY9407_1	0°S - 3°S	142°E - 143°E	Aug 1994	7
FLUPAC	West Pacific 35A319940923	0°S - 15°S	165°E - 167°E	Sep 1994 - Oct 1994	66
Section I8S/I9S	Indian Ocean 316N145_5	32°S - 45°S	95°E - 115°E	Dec 1994 - Jan 1995	29
Section I9N	Indian Ocean 316N145_6	0°S - 32°S	93°E - 106°E	Jan 1995 - Feb 1995	100
Section SR3	Southern Ocean AR9404_1	44°S - 45°S	146°E - 147°E	Jan 1995 - Feb 1995	5
Section I8N/I5E	Indian Ocean 316N145_7	31°S - 34°S	91°E - 115°E	Apr 1995	57
Section I3	Indian Ocean 316N145_8	20°S - 22°S	90°E - 114°E	Apr 1995 - May 1995	31
Section	West Pacific 49HG19950414	1°S - 35°S	153°E - 163°E	Apr 1995 - May 1995	25
Section I4	Indian Ocean 3175MB95_07	31°S - 43°S	90°E - 110°E	Sep 1995 - Oct 1995	28
Section I10	Indian Ocean 316N145_13	9°S - 25°S	106°E - 112°E	Nov 1995	76
Section I2	Indian Ocean 316N145_14_15	8°S - 9°S	90°E - 106°E	Dec 1995	37
Section SR3	Southern Ocean 09AR19960822	44°S - 45°S	146°E - 147°E	Sep 1996 - Oct 1996	5
Section I2	Indian Ocean 09AR20000927	28°S - 34°S	94°E - 115°E	Sep 2000 - Nov 2000	66
Section SR3	Southern Ocean 09AR20011029	44°S - 45°S	146°E - 147°E	Oct 2001	7
Section I5	Indian Ocean 74AB20020301	31°S - 35°S	91°E - 115°E	Apr 2002	34
OISO-10	Southern Ocean 35MF20030123	45°S	146°E	Jan 2003	5
Section P6W	West Pacific 49NZ20030803	30°S	154°E - 170°E	Aug 2003	40
Section I3	Indian Ocean 49NZ20031209	20°S - 22°S	90°E - 113°E	Jan 2004	33
Section I9S	Southern Ocean I09S_09AR20041	35°S - 44°S	115°E	Dec 2004	18
Section P10	West Pacific 49NZ20050525	0°S - 4°S	145°E - 146°E	Jun 2005	18
TransFuture 5	Tasman Sea/ Coral Sea	10°S - 40°S	144°E - 172°E	Feb 2007 - Sep 2011	1460
Section I8S	Indian Ocean I08S_33RR20070	28°S - 45°S	94°E - 95°E	Mar 2007	79
Section I9N	Indian Ocean I09N_33RR20070	0°S - 28°S	93°E - 95°E	Mar 2007 - Apr 2007	103
Section I5	Indian Ocean I05_33RR200903	31°S - 35°S	90°E - 115°E	Apr 2009 - May 2009	128
Section P21	West Pacific 49NZ20090521	18°S - 25°S	154°E - 170°E	Jun 2009	52

Section P6W	West Pacific 318M20091121	30°S	154°E - 170°E	Nov 2009 - Dec 2009	93
SS201004	Indian Ocean	21°S - 23°S	112°E - 115°E	May 2010	92
Total					2772

[1] http://cdiac.ornl.gov/ftp/oceans/

Table 1. Cruise data used to derive the salinity versus total alkalinity relationship for surface waters in Australian regional seas.

	Lat	Lon	SST - *BIAS*	SST - *R*	OmA - *BIAS*	OmA -*R*	n
Esperance	33° 56S	121°51E	0.8	0.93	0.09	-0.06	16
Kangaroo Island	35° 49S	136° 27E	0.38	0.84	0.01	0.03	27
Maria Is	42° 36	148° 14E	0.6	0.93	0.07	0.83	40
Rottnest Is	32° 25S	115° 25S	1.01	0.92	0.06	0.26	33
Ningaloo	21° 52S	113° 57S	0.08	0.95	0.17	0.62	11
Yongala	19° 19S	147° 27S	0.13	0.94	0.27	0.45	37
Port Hacking	34° 5S	151° 6S	0.82	0.89	0.09	0.58	46
North Stradbroke	27° 18S	153° 6S	0.08	0.96	0.06	0.78	40

Table 2: The locations of the NRS sites used in this study, along with the biases, correlation coefficient (*R*) between the SST and aragonite saturation state observed at the site with values from our reconstruction, HadSST and calculated omega, respectively. Also listed are the number of observations used in calculating the Biases and Correlations